ISSN 0036-0244, Russian Journal of Physical Chemistry A, 2011, Vol. 85, No. 2, pp. 264–273. © Pleiades Publishing, Ltd., 2011.
Original Russian Text © L.S. Sosenkova, E.M. Egorova, 2011, published in Zhurnal Fizicheskoi Khimii, 2011, Vol. 85, No. 2, pp. 317–326.

PHYSICAL CHEMISTRY OF NANOCLUSTERS AND NANOMATERIALS

Small-Sized Silver Nanoparticles for Studies of Biological Effects[1]

L. S. Sosenkova and E. M. Egorova

Laboratory of Nanopathology, Institute of General Pathology and Pathophysiology, Russian Academy of Medical Sciences, ul. Baltiiskaya 8, Moscow, 125315 Russia
e-mail: lubasya@inbox.ru

Received January 29, 2010

Abstract—The influence of the hydration extent, AOT and silver ion concentration on average particle size and size distribution in micellar solution of silver nanoparticles obtained by biochemical synthesis was investigated. Formation and stability of nanoparticles were controlled by measurements of optical absorption spectra. Particle sizes were determined by transmission electron microscopy. Combinations of varied parameters have been found, making it possible to prepare three micellar solutions of spherical silver nanoparticles with a different average size in the range 4.6–10.5 nm and narrow size distribution (the standard deviation does not exceed 2.5 nm). For the water dispersions prepared from such solutions by the specially developed procedure, possible applications for studies of size effects in the biological action of nanoparticles are also discussed.

Keywords: silver nanoparticles, biochemical synthesis, reverse micelles.

DOI: 10.1134/S0036024411020324

INTRODUCTION

Intensive studies on the properties of nanoparticles and nanomaterials, as well as the development of various practical applications, may be regarded as a prominent feature of the last decade. Metal nanoparticles represent one of the most popular objects, which have already found application in chemistry, engineering, and medicine. Among medical applications, the most known are the improvements in diagnostics and healing of various (including oncological) diseases with the use of gold nanoparticles [1–5], as well as antimicrobial means in the form of colloidal solutions, or liquid-phase and solid materials containing silver nanoparticles [6–9]. Silver nanoparticles exhibit the widest spectrum of applications, the fact that has stimulated intensive studies of their biological effects. The main goal of such studies is accumulation of the data on the degree of toxicity of these nanoparticles to living organisms, which makes it possible to define conditions for their safe use.

The biological action of silver nanoparticles was studied on the objects of different type: on bacteria and viruses [10–18], algae [19], animal and human cultured cells [20–22], fish embryos [23], and animal organisms [24, 25]. In all cases, silver nanoparticles manifest themselves as a toxic agent causing more or less obvious suppression of live functions, up to the destruction (cells and embryos) or disturbance of the normal functioning of certain organs (for animal organisms). The intensity of toxic action depended primarily on the nanoparticle concentration in the environment. The threshold concentrations, which marked the beginning of toxic effects, depended on the object type. It has also been revealed that the degree of toxicity of nanoparticles is sensitive to their size and shape: for one and the same way of preparation and at a given concentration in the environment, 9-nm nanoparticles appeared to be more toxic than those 60 nm in size [14], and triangular particles are more toxic than spherical ones [15].

In our studies of the biological action both of silver nanoparticles in water solutions and materials modified by these nanoparticles, it was shown that they behave as a strong toxic agent suppressing viability of various microorganisms (bacteria and viruses) [6, 26], slime mold [27, 28], unicellular alga [29], and plant seeds and mammalian organisms [29, 30]. The concentration ranges where the nanoparticles do not exert their toxic action were defined.

The experiments were carried out with 9 ± 6 nm nanoparticles obtained by the biochemical synthesis [31, 32]. The method is based on reduction of metal ions by natural plant pigments (flavonoids) in reverse micelles formed by an anionic surfactant. As shown earlier [6, 32–34], the method allows us to obtain nanoparticles of various metals (including silver) small in size and stable in a reverse-micellar (referred to further as micellar) solution for a long time. Therefore, it is possible to carry out systematic investigations of their properties and develop various ways for their practical application. From their micellar solutions, water dispersions of silver nanoparticles are prepared

[1] The article was translated by the authors.

by a specially developed procedure [35]; these water dispersions may be used, in particular, for studying interaction of nanoparticles with biological objects. It is assumed that development of these studies will be in the two main directions: (1) widening the range of biological objects and (2) variation of particle parameters (size, shape, and surface charge) essential for their biological action.

Here, we report the results of our work aimed at obtaining silver nanoparticles (SNPs) of different average diameter with narrow size distribution, in order to study the dependence of their biological effect on particle size. It was important, as we believed, to investigate the region of small sizes (below 20 nm), where the so-called "size effects" are most distinctly expressed [1, 36]. Hence, we may expect that exactly in this size range the effect of particle size will be most distinctly expressed. To achieve our goal we varied three parameters of the reverse-micellar system: the concentration of stabilizer (AOT), that of silver ions, and the hydration extent $w = [H_2O]/[AOT]$. As reported earlier in a series of works devoted to the studies of metal nanoparticles formation in reverse micelles (e.g., [37–42]), these parameters affect the sizes of water micelles and/or nanoparticles. As will be shown below, we managed to find the combinations of parameters providing that at least two populations of spherical silver nanoparticles are formed with rather narrow distribution and large enough difference in the average sizes, the maximum average size not exceeding 10.5 nm. The formation process and stability of nanoparticles were controlled by measurements of optical absorption spectra. Particle sizes were determined by transmission electron microscopy.

EXPERIMENTAL

Silver nitrate (analytical grade) and deionized water (no less than 10 MΩ) obtained from Vodolei water purification system (Khimelectronika, Moscow, Russia) were used to prepare the $AgNO_3$ aqueous solution. The complex silver salt $[Ag(NH_3)_2]NO_3$ was prepared by adding 27% aqueous ammonium hydroxyde to the silver nitrate water solution. To prepare quercetin micellar solutions, AOT (sodium bis(2-dioctyl)sulphosuccinate, Aldrich or Acros) (≥96%, Fluka), isooctane (analytical grade) and quercetin (3,5,7,3',4'-pentahydroxyflavon, Merck) were used.

The standard procedure for preparing the quercetin (Qr) micellar solution is described in detail elsewhere [32, 33, 43]. Briefly, Qr taken as a powder was solubilized in the preliminary prepared AOT solution in isooctane. The Qr concentration in micellar solution was determined as described in [43].

For the synthesis of silver nanoparticles, an $[Ag(NH_3)_2]NO_3$ water solution was added to the 2.65×10^{-4} M Qr micellar solution to the concentration, $C_{Ag} = (1–7.4) \times 10^{-3}$ M and hydration extent, $w = [H_2O]/[AOT] = 3.7$, 5, or 10. The AOT concentration in the micellar solution (C_{AOT}) was varied in the range 0.015–0.135 M. The concentration of silver nanoparticles (C_{SNP}) in the micellar solution was determined from the measured optical densities in the absorption band maximum and the extinction coefficient ($\varepsilon = 1.03 \times 10^4$ l/(mol cm)) found by us as described in [43].

The absorption spectra of micellar or water solutions were recorded on a Helios-α spectrophotometer (Thermo Electronics, GB) in a 1-mm quartz cell at room temperature. Either isooctane or distilled water was used as reference solution. Particle sizes in micellar solutions were determined by transmission electron microscopy on a LEO912 AB OMEGA microscope (Carl Zeiss, Germany) at an accelerating voltage 120 kV. From electron micrographs, the particle size distributions were found for no less than 350 particles. Average sizes and standard deviations were determined using the Gauss approximation.

RESULTS AND DISCUSSION

As shown earlier [32, 33, 43], the introduction of silver salt water solution to the Qr micellar solution leads to rapid changes in color and absorption spectrum. The colorless or light-yellow quercetin solution becomes red-brown or almost black depending on the nanoparticle concentration. Figure 1 shows the typical change in the absorption spectra of the Qr micellar solution after the addition of $[Ag(NH_3)_2]NO_3$ water solution in the standard synthesis procedure. Instead of the two-band spectrum in the UV region characteristic of flavonoids [44–46], a new absorption band appears with $D_{max} = 420–440$ nm, lying in the range characteristic for silver nanoparticles in reverse micelles at a low hydration extent [42, 47]. The optical density in the band maximum (D_{max}) allows us to find the SNP concentration at the given time after the beginning of synthesis. The completion of nanoparticle formation corresponds to the stationary stage when the D_{max} value remains nearly constant. The rate of SNP formation depends on the salt silver concentration. As seen from Fig. 1, at $c_{Ag} = 7.4$ mM the process is almost fully accomplished within 2 h, when D_{max} reaches its stationary value. After the stationary state is established, only small changes of optical density take place, not exceeding 10% of the D_{max}. At the smaller silver concentrations, the process can be slowed down, but in all investigated cases, the formation of nanoparticles is finished in no more than 1–2 days. The SNP concentration at the stationary stage (c_{NP}) depends on the system parameters; in the case shown in Fig. 1, $c_{NP} = 3.84$ mg-ion Ag^+/l or 0.40 g/l (recalculated to metal silver). For the particle size measurements, the solutions were used taken at the stationary stage, 7 days after the beginning of synthesis.

The electron micrograph and size distribution in SNP micellar solutions, obtained at the parameters given in the legend to Fig. 1, are presented in Fig. 2.

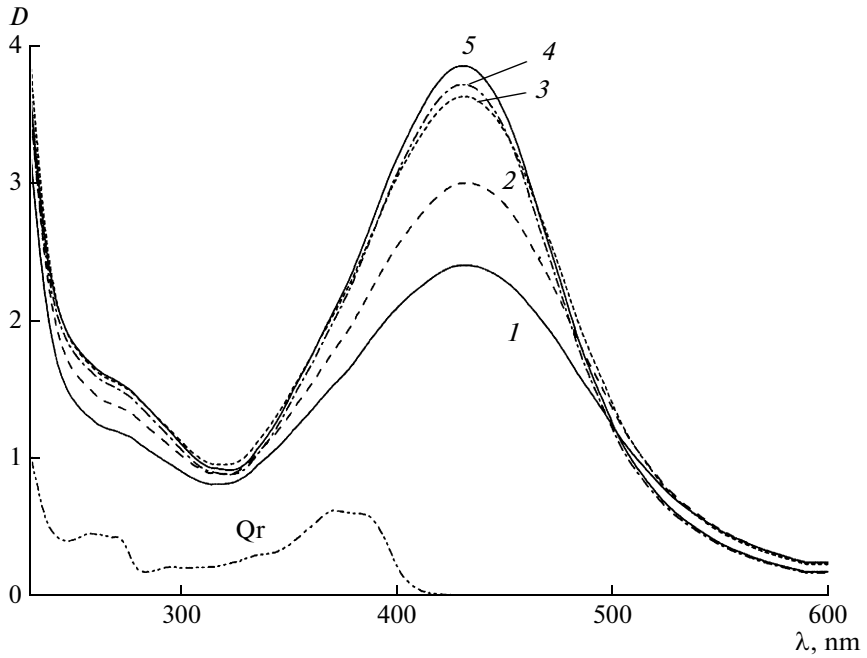

Fig. 1. Formation kinetics of Ag nanoparticles. Silver ion concentration in micellar solution, $c_{Ag} = 7.4$ mM; $w = 3.7$, $c_{AOT} = 0.135$ M. Quercetin concentration here and in the other experiments, $c_{Qr} = 2.65 \times 10^{-4}$ M. Absorption spectra are measured 5 min (*1*), 30 min (*2*), 2 h (*3*), 1 day (*4*), and 7 days (*5*) after the addition of silver salt water solution (beginning of synthesis).

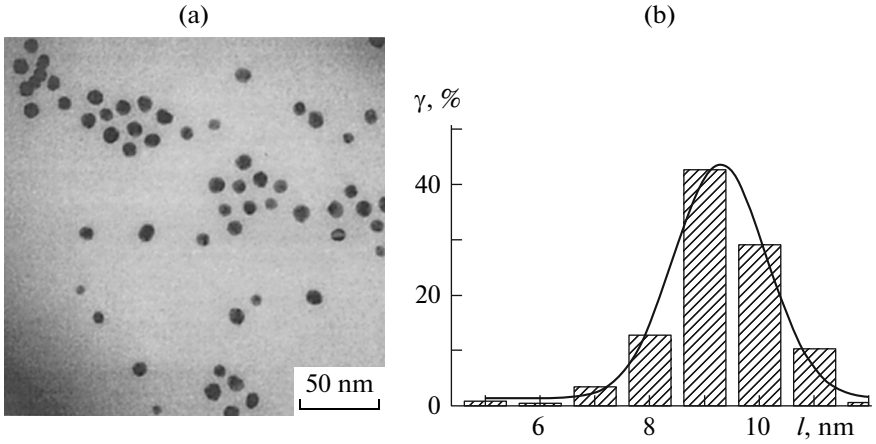

Fig. 2. Electron micrograph (a) and particle size distribution (b) in micellar solution of Ag nanoparticles at $w = 3.7$, $c_{Ag} = 7.4$ mM, $c_{AOT} = 0.135$ M. Average particle size; $d_{av} = 9.3$ nm, standard deviation, $\Delta = \pm 1.7$ nm. Here and in Figs. 4, 6, 8, and 10, the micrographs are obtained 7 days after the beginning of synthesis. l—particle size (nm), γ—fraction of the particles.

The nanoparticles are spherical, with average size $d_{av} =$ 9.3 nm and standard deviation $\Delta = \pm 1.7$ nm.

To change the particle average size, we varied successively three parameters of the reverse-micellar system: the AOT concentration (c_{AOT}), that of silver salt (c_{Ag}) and the hydration extent *w*. As known from literature, and *w* value affect the size of the micelle water core [37, 39, 40], where metal ions are reduced with subsequent formation of the particles containing small number of silver atoms (nanoclusters). Variation of silver salt concentration causes changes in the particle size because of the changes in the aggregation rate of the nanoclusters [41, 42].

The AOT concentration was changed to the smaller values as it enabled us further to decrease the surfactant concentration in the SNP water solutions, this may be essential for the studies of their action on biological objects in the water media. Figure 3 shows the spectra of SNP micellar solutions, obtained at the same *w* and c_{Ag} values but at different AOT concentrations: $c_{AOT} = 0.135$ M (the standard value), 0.08 and 0.042 M. It is seen that the decrease of c_{AOT} results in

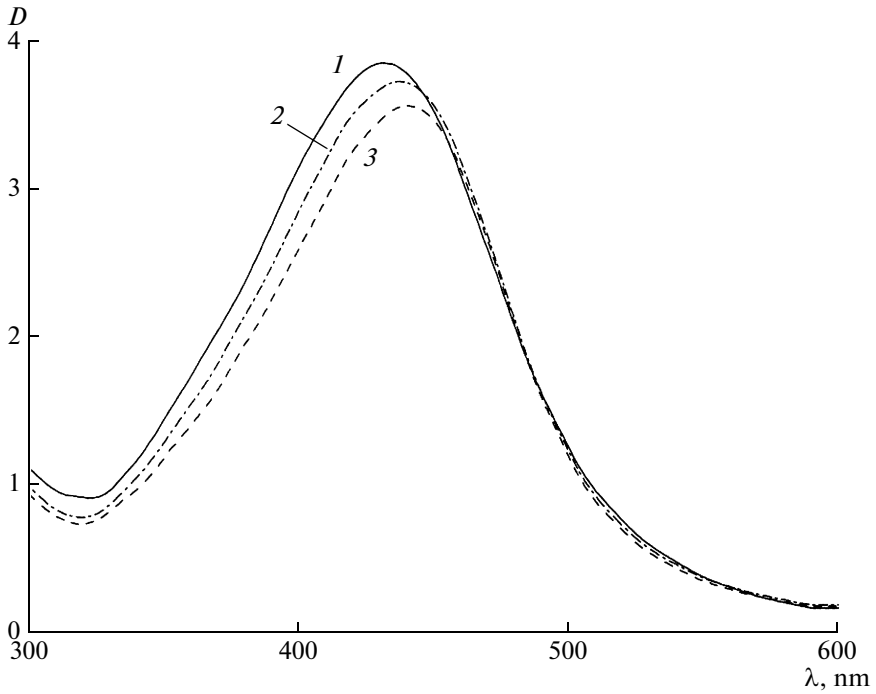

Fig. 3. The effect of AOT concentration on formation of Ag nanoparticles. Parameters of micellar solution: $c_{Ag} = 7.4$ mM, $w = 3.7$, c_{AOT} (M): 0.135 (*1*), 0.08 (*2*) and 0.042 (*3*). Spectra here and in Figs. 5, 7, and 9 are measured 7 days after the beginning of synthesis.

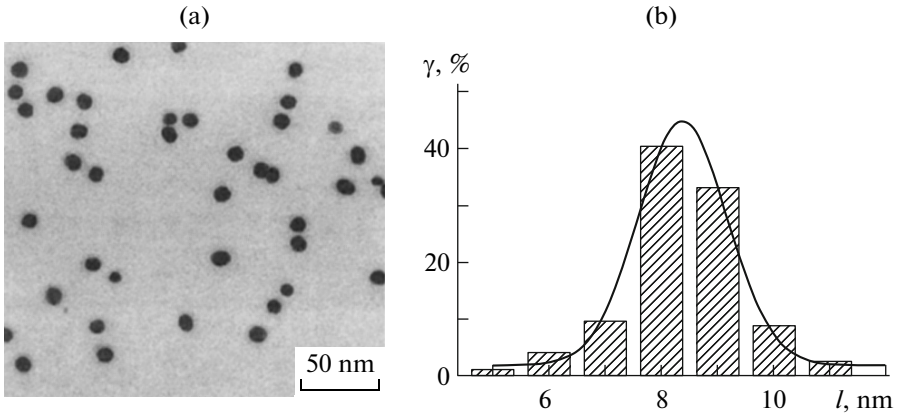

Fig. 4. Electron micrograph (a) and particle size distribution (b) in SNP micellar solution at $w = 3.7$, $c_{Ag} = 7.4$ mM, $c_{AOT} = 0.08$ M, $d_{av} = 8.4$ nm, $\Delta = \pm 1.6$ nm.

the insignificant fall of SNP concentration (D_{max} values), more noticeable for the smallest AOT concentration. In addition, a small shift of the absorption band to the long waves (from 433 to 440 nm) is observed, identical for the two last C_{AOT} values. According to the known Mie theory, this may indicate to the increase in the average particle size [47, 48].

To determine particle sizes, we used the solution with $c_{AOT} = 0.08$ M, because in this case, at the same supposed increase in size, there remains a higher nanoparticle concentration. Figure 4 shows an electron micrograph and size distribution for the solution with $c_{AOT} = 0.08$ M. Here, the average size appeared to be 8.4 nm, that is, somewhat smaller than at $c_{AOT} =$ 0.135 M (9.3 nm), with almost the same standard deviation (1.6 and 1.7 nm, respectively). Thus, for an AOT concentration approximately 1.7 times smaller, we have obtained a SNP solution with an average size only slightly different from that in the standard solution. It is clear also that in this case, the assumption about the increase in size, issuing from the red shift of the absorption band, is not confirmed by the electron microscopy data.

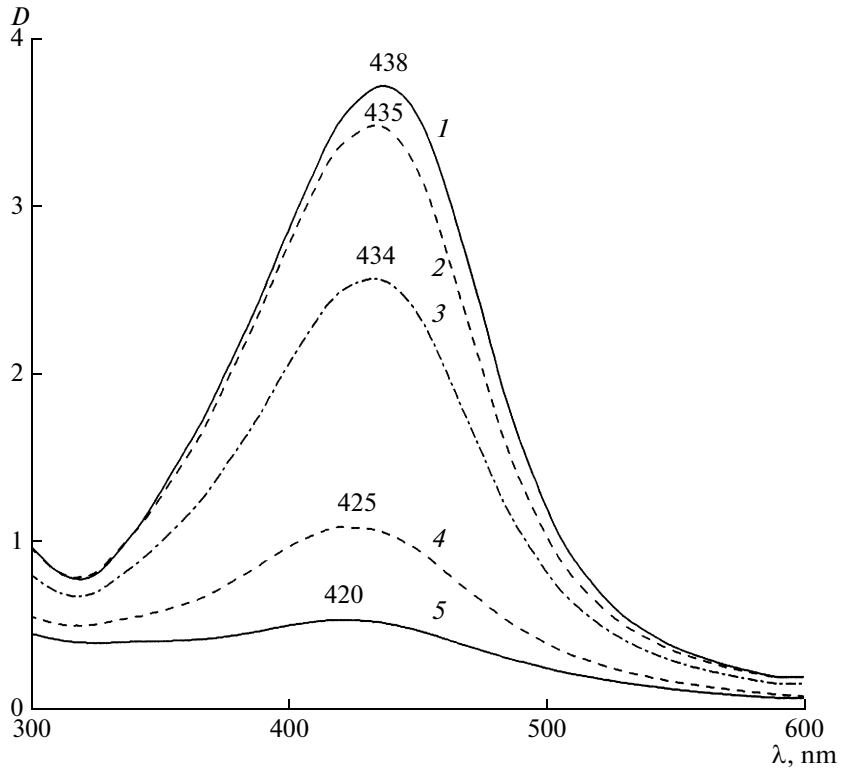

Fig. 5. Effect of silver concentration on the formation of nanoparticles. Parameters of micellar solution: $w = 3.7$, $c_{AOT} = 0.08$ M, c_{Ag} (mM): 7.4 (*1*), 4 (*2*), 2.4 M (*3*), 1 (*4*), 0.5 (*5*). Figures on curves show wavelengths of absorption band maxima.

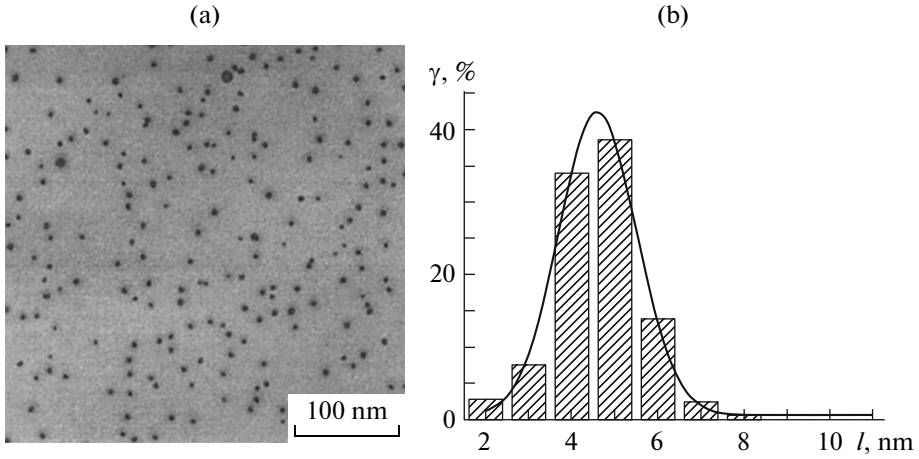

Fig. 6. Electron micrograph (a) and size distribution (b) in SNP micellar solution at $w = 3.7$, $c_{Ag} = 1$ mM, $c_{AOT} = 0.08$ M, $d_{av} = 4.6$ nm, $\Delta = \pm 1.8$ nm.

The decrease of silver salt concentration in the range 7.4–0.5 mM leads to the essential decrease of SNP concentration and to a shift in the band maximum towards short wavelengths (Fig. 5). For electron microscopy, we have chosen the SNP synthesized at $c_{Ag} = 1$ mM, since here the noticeable shift of λ_{max} is observed (hence it is possible to assume the significant decrease of the particle size), and at the same time the SNP concentration is not too low. The electron micrograph and particle size distribution in this SNP micellar solution are shown in Fig. 6. It turned out that here the decrease in silver concentration (in this case, in accordance with the Mie theory) actually leads to a decrease in the average particle size to 4.6 nm at almost the same standard deviation (±1.8 nm). Thus, we obtained an SNP solution with particles almost

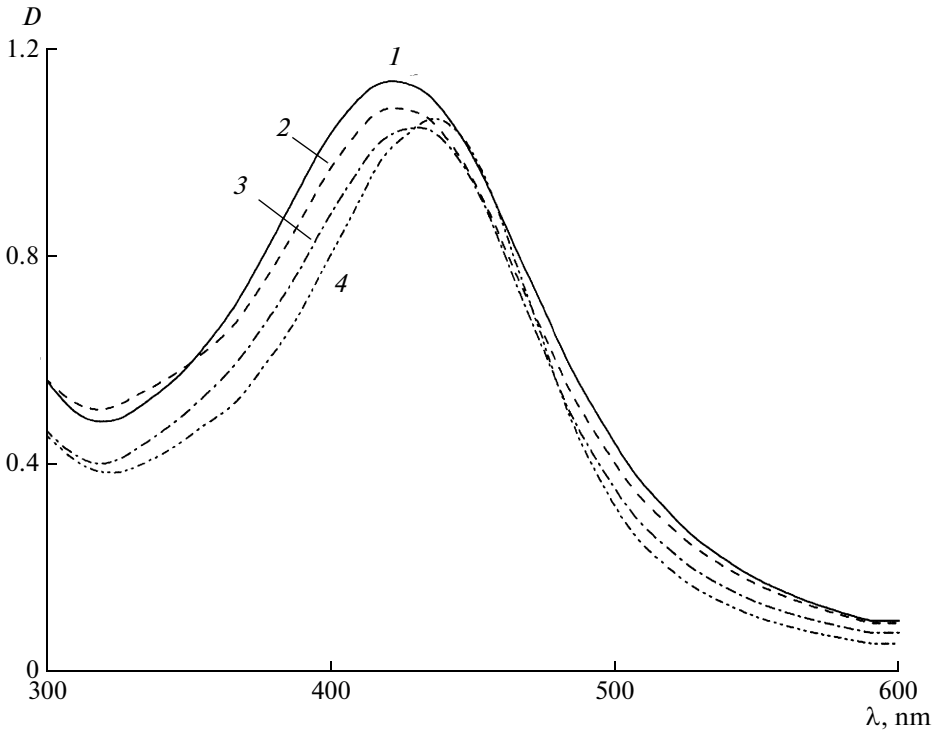

Fig. 7. Influence of AOT concentration on nanoparticle formation. Parameters of micellar solution: c_{Ag} = 1 mM, w = 3.7, c_{AOT} (M): 0.135 (*1*), 0.08 (*2*), 0.04 (*3*), 0.015 (*4*).

two times smaller than those in solutions with c_{Ag} = 7.4 mM.

Further we found it useful to elucidate whether the AOT concentration exerts an influence on the particle sizes for the solution with c_{Ag} = 1 mM, that is, whether the results of the preceding experiment are conditioned by the fact that the effect of AOT concentration cannot be revealed at a large concentration of silver ions. Such a supposition issues from the following reasons. It is obvious that the higher silver ion concentration, the greater the rate of nanoparticle formation and aggregation. The influence of AOT concentration on the aggregation process may manifest itself in the fact that the AOT molecules adsorbed on the surface of nanoparticles prevent them from aggregating and thus decrease the particle average size. The rate of AOT adsorption will be higher, the greater its concentration; therefore, the increase in AOT concentration should lead to a decrease in the average particle size. However, such an effect can be clearly expressed when the AOT adsorption rate is comparable to that of nanoparticle aggregation, i.e., when the concentration of silver ions is not too high.

Figure 7 shows changes in the absorption spectra with AOT concentration changes in solutions with c_{Ag} = 1 mM. Similarly to what is found for the greater concentration of silver ions (Fig. 3), here the shift of the absorption band to bigger wavelengths is observed, which is the greater, the smaller the AOT concentration; the maximal shift (at c_{AOT} = 0.015 M) is 15 nm. The electron micrograph for the solution with c_{AOT} = 0.015 M is given in Fig. 8. From histogram analysis, we find $d_{av} = 7.7 \pm 1.13$ nm, that is, an obvious increase in the average size in comparison with the solution with c_{AOT} = 0.08 M (Fig. 6). Hence, it follows that the particle average size can be increased by decreasing the AOT concentration, but this parameter works at a sufficiently small concentration of silver ions. It is possible that in this case the shift in the SNP absorption band position to the long waves reflects the increase in the particle size, in agreement with the Mie theory predictions.

Thus, at the given stage of research, we obtain three SNP solutions with close average particle sizes (7.7–9.3 nm) and one solution with an average size of 4.6 nm, i.e., 1.7–2 times smaller. The standard deviation for all solutions does not exceed 1.8 nm.

The effect of hydration extent was studied in solutions with c_{Ag} = 1 mM, c_{AOT} = 0.08 M. Figure 9 shows the spectra of SNP solutions prepared at three values of hydration extent: w = 3.7, 5, and 10. It is seen that the increase in w in this range has practically no influence on the SNP concentration, but it results in a blue shift of the absorption band by 6–7 nm. According to the Mie theory, such a shift can be caused by the decrease in particle size. However, in this case, such a decrease seems to hardly possible since it is well known that, in metal nanoparticle synthesis in reverse

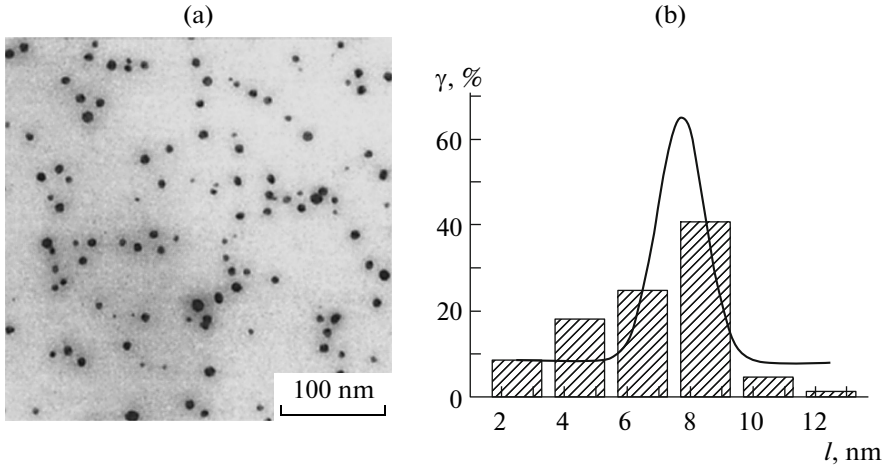

Fig. 8. Electron micrograph (a) and size distribution (b) in SNP micellar solution at $w = 3.7$, $c_{Ag} = 1$ mM, $c_{AOT} = 0.015$ M, $d_{av} = 7.7$ nm, $\Delta = \pm 1.13$ nm.

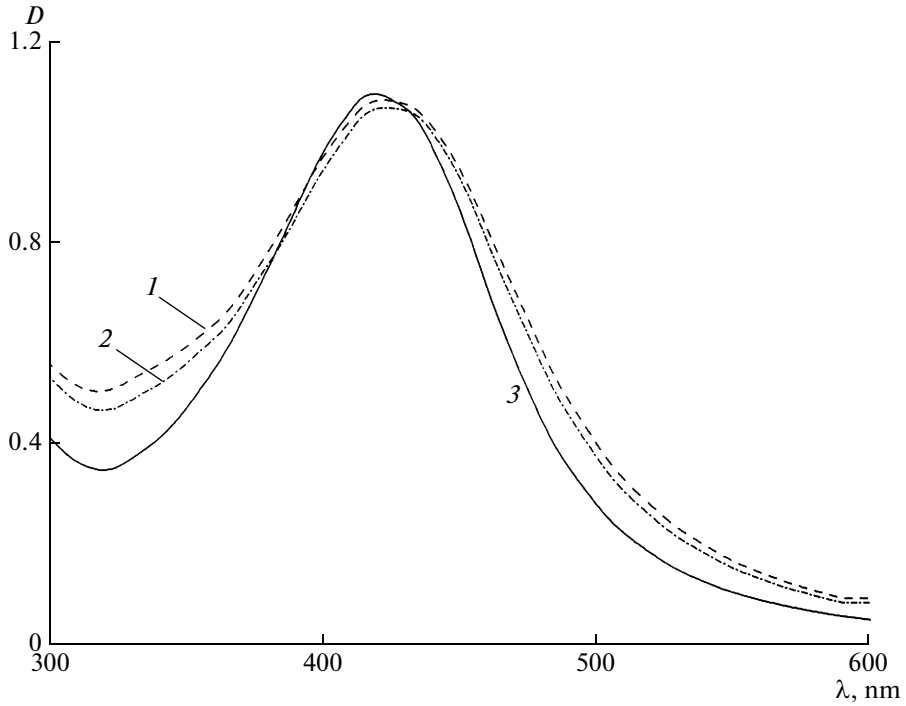

Fig. 9. Effect of hydration extent on nanoparticle formation. Parameters of micellar solution: $c_{Ag} = 1$ mM, $c_{AOT} = 0.08$ M, $w = 3.7$ (*1*), 5 (*2*), and 10 (*3*).

micelles, the increase in w, on the contrary, leads to an increase in particle size (e.g., [38, 41, 42, 49]). The same effect of the increase in the hydration extent is observed in our case. An electron micrograph and the particle size distribution in solution at $w = 10$ are presented in Fig. 10. In comparison with the solution at $w = 3.7$, the average size has become almost three times as large, 10.35 nm; however, the size dispersion has also increased, since the standard deviation is 2.5 nm. A similar tendency toward an increase in the degree of polydispersion with an increased hydration extent for SNP micellar solutions was also observed by other authors [41]. As supposed in [41], this may be related to the increase in the size of the micelle water core, which leads to an increase in the fraction of less rigidly structured water and, consequently, to facilitation of the exchange of micelle content by impacts. As a result, the frequency of impacts, mergings, and splittings of micelles increases with nanoparticle growth, with a corresponding increase in the width of their size distribution.

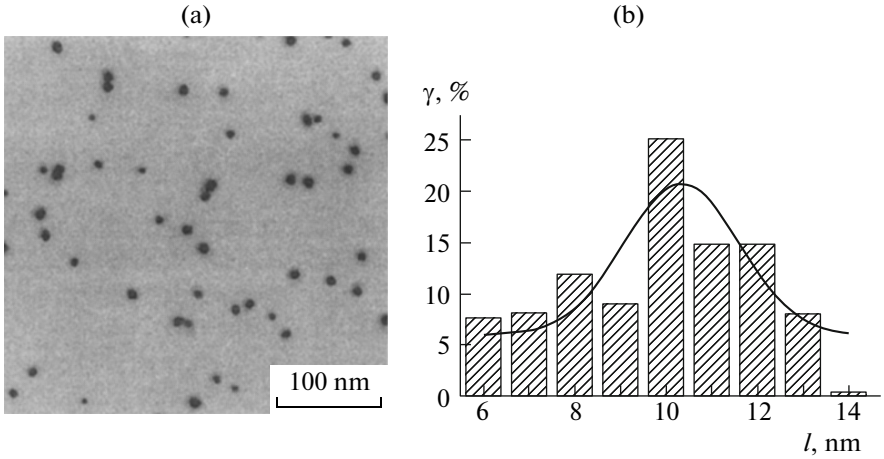

Fig. 10. Electron micrograph (a) and size distribution (b) in SNP micellar solution at $w = 10$, $c_{Ag} = 1$ mM, $c_{AOT} = 0.08$ M, $d_{av} = 10.35$ nm, $\Delta = \pm 2.5$ nm..

The whole series of sizes obtained by us, with the relevant nanoparticle concentrations and other parameters of micellar solutions, are presented in the table.

It is known that, during their transfer to the water phase, the sizes of nanoparticles do not change and their concentration appears to be equal or close to that in the micellar solution [29, 35]. Therefore, from the data given in the table, it is possible to make conclusions on the applicability of various variants of synthesis (N 1–5) for studying biological effects of nanoparticles in water media.

Variants 1 and 2 give nanoparticles of both nearly equal size (with small dispersion) and concentration in solution. They differ only in AOT concentration. Our way of preparing SNP water solutions is described in [35]. Since in the thus obtained water solution the AOT concentration is the lesser, the smaller its concentration in the initial micellar solution [29], the choice between these two variants can be made judging from the significance of the value of AOT concentration for the object studied, when this surfactant is introduced into the experimental system with the SNP solution. As follows from our experimental practice [6, 29], in the tests on water suspensions of bacterial cells, the bactericidal action of silver nanoparticles is manifested at such high dilutions (50 times or more) that the presence of AOT in both variants cannot have an effect on the object under study. So it is possible to use both variants of synthesis. If, for the dilutions used, in variant 1 the toxic action of AOT is detected in the control experiments (the introduction of AOT water solution in the absence of nanoparticles), then variant 2 is preferable. If it is necessary to provide a high concentration of nanoparticles in the medium and variant 2 is not applicable because of the toxicity of AOT, it is possible to use variant 3, where the AOT concentration in water solution is approximately one order less than in variant 1.

For comparison of action of nanoparticles of different size, it is possible to use variants 4 and 2, 4 and 5, or 4 and 3. It is also necessary to keep in mind that, as mentioned above, apart from particle size, an essential role in SNP biological action can be played by their adsorption on a cell membrane, which depends on the numerical concentration of nanoparticles (i.e., the number of particles per unit volume in solution, c^*_{NP}) added to the experimental system. Therefore, for correct determination of the effect of particle size, it is important that, for nanoparticles of different size, the c^*_{NP} values be identical in the experimental system.

Correspondingly, if the study is performed with two water solutions containing nanoparticles of different size and the initial c^*_{NP} values, it is necessary to use different degrees of dilution in order to ensure equal numerical nanoparticles concentration in the experimental system. As seen from the data of our table, if the effects of solutions 4 and 2, with different particle sizes and equal initial c^*_{NP} values, are compared, for example, on a cell culture, it is possible to use one and the same dilution of the initial SNP water solutions. If the biological effects of variants 4 and 5 are compared, it is necessary to use for solution 5 an SNP

Particle sizes and concentrations, AOT concentrations, and degrees of hydration in micellar solutions of silver nanoparticles

No.	d_{av}, nm	Δ, nm	c_{AOT}, M	w	c_{NP}, g/l	c^*_{NP}, particles/ml
1	9.3	1.7	0.135	3.7	0.40	9.1E+13
2	8.4	1.6	0.08	3.7	0.39	1.2E+14
3	7.7	1.13	0.015	3.7	0.11	4.4E+13
4	4.6	1.8	0.08	3.7	0.11	2.1E+14
5	10.35	2.5	0.08	10	0.11	1.8E+13

concentration in the experimental system that is ten times higher (the dilution, ten times less), since the initial ±1.13 value in solution 5 is ten times smaller than in solution 4. A similar correction should be made in comparing solutions 4 and 3.

To summarize, it is possible to conclude that biochemical synthesis allows one to obtain solutions of silver nanoparticles with an average size in the range 4.6–10.5 nm with a narrow size distribution (with a standard deviation $\Delta = 1.13–2.5$ nm). All of the nanoparticles are approximately spherical and stable in solution for a long time (up to several years). The change in particle sizes is achieved by variation of the parameters of the reverse-micellar system where the synthesis is conducted, namely, of the AOT and silver concentration, and of the hydration extent. It is necessary to note that changes in the position of the absorption band maximum, observed with a change in the chosen parameter do not always agree with Mie theory predictions. Hence, it follows that, in the investigated system, apart from size changes, a shift of the SNP absorption band can result from the other factors. As reported in a number works devoted to studies of the optical properties of silver nanoparticles ([50–52] and references therein), such factors can be the adsorption of molecules or ions present in a solution (in our case, probably, silver ions) on the SNP surface, as well as the adsorption of nanoparticles on silver oxide microcrystals. Further studies will be devoted to elucidating the reasons for the nanoparticle band shift in cases when disagreement with the Mie theory is observed. It is also supposed that selection of the combinations of system parameters will make it possible to prepare solutions with an average particle size in the range of 10–20 nm and then to implement systematic studies of the role of particle sizes in the biological effects of silver nanoparticles.

ACKNOWLEDGMENTS

The authors are grateful to Dr. S.S. Abramchuk from Moscow State University for his assistance in making electron micrographs of silver nanoparticles in micellar solutions.

REFERENCES

1. A. D. Pomogailo, A. S. Rozenberg, and I. E. Uflyand, *Nanoscale Metal Particles in Polymers* (Khimiya, Moscow, 2000) [in Russian].
2. X. Huang, P. K. Jain, I. H. El-Sayed, and M. A. El-Sayed, Nanomedicine **2**, 681 (2007).
3. D. Pissuwan, S. M. Valenzuela, and M. B. Cortie, Trends Biotechnol. **24**, 62 (2006).
4. P. Mukherjee, R. Bhattacharya, N. Bone, et al., J. Nanobiotechnology **5** (4) (2007), doi:10.1186/1477-3155-5-4.
5. S. Norman, J. W. Stone, A. Gole, et al., Nano Lett. **8**, 302 (2008).
6. E. M. Egorova, Nanotekhnika, No. 1, 15 (2004).
7. R. P. Evstigneeva and V. P. Pchelkin, Khim.-Farmats. Zh. **40**, 34 (2006).
8. O. V. Salata, J. Nanobiotechnol. **2** (3) (2004), doi:10.1186/1477-3155-2-3.
9. M. E. Stratmeyer, P. L. Goering, V. M. Hitchins, et al., Biomed. Microdevices (2008), doi 10.1007/s10544-008-9261-9.
10. L. A. Koulskii, *Silver Water* (Naukova Dumka, Kiev, 1987) [in Russian].
11. A. N. Lopanov, *Silver* (Agat, St. Petersburg, 2005) [in Russian].
12. V. I. Karamushka, D. M. Gadd, T. G. Gruzina, and Z. R. Ulberg, Kolloidn. Zh. **60**, 775 (1998) [Colloid. J. **60**, 717 (1998)].
13. I. Sondi and B. Salopek-Sondi, J. Colloid Interface Sci. **275**, 177 (2004).
14. C.-N. Lok, C.-M. Ho, R. Chen, et al., J. Biol. Inorg. Chem. **12**, 527 (2007).
15. S. Pal, Y. K. Tak, and J. M. Song, Appl. Environm. Microbiol. **73**, 1712 (2007).
16. J. S. Kim, E. Kuk, K. N. Yu, et al., Nanomed.: Nanotechnol. Biol. Med. **2**, 95 (2007).
17. J. L. Elechiguerra, J. L. Burt, J. R. Morones, et al., J. Nanobiotechnol. **3** (6) (2005), doi:10.1186/1477-3155-3-6.
18. A. L. Neal, Ecotoxicology **17**, 362 (2008).
19. Z. R. Ulberg, L. G. Marochko, A. G. Savkin, and N. V. Pertsov, Kolloidn. Zh. **60** (1998) [Colloid. J. **60**, 775 (1998)].
20. L. Braydich-Stolle, S. Hussain, J. J. Schlager, and M.-C. Hofmann, Toxicol. Sci. **88**, 412 (2005).
21. S. Hussain, K. Hess, J. Gearhart, et al., Toxicol. Sci. **92**, 456 (2006).
22. S. Sheikpranbabu, K. Kalishwaralal, D. Venkataraman, et al., J. Nanobiotechnol. **7** (8) (2009), doi:10.1186/1477-1355-7-8.
23. P. V. Asharani, Y. L. Wu, Z. Gong, and S. Valivaveettil, Nanotecnology **19**, 255102 (2008).
24. J. H. Ji, J. H. Jung, S. S. Kim, et al., Inhalat. Toxicol. **19**, 857 (2008).
25. Y. S. Kim, J. S. Kim, H. S. Cho, et al., Inhalat. Toxicol. **20**, 575 (2008).
26. L. N. Shirokova, V. A. Aleksandrova, E. M. Egorova, and G. A. Vikhoreva, Prikl. Biokhim. Mikrobiol. **45**, 422 (2009).
27. N. B. Matveeva, E. M. Egorova, S. I. Beylina, and V. V. Lednev, Biofizika **51**, 859 (2006) [Biophysics **51**, 758 (2006)].
28. N. B. Matveeva, E. M. Egorova, and S. I. Beylina, Pushchino, 240–242 (2008).
29. E. M. Egorova, (Nova Sci., New York, USA, 2010, in press).
30. L. K. Ramayya, K. G. Ordzhonikidze, E. M. Egorova, and A. V. Rubanovich, Acta Naturae, No. 3, (2009).
31. E. M. Egorova, A. A. Revina, and V. S. Kondratieva, Patent RF No. 2147487.
32. E. M. Egorova and A. A. Revina, Colloids Surf. A **168**, 87 (2000).
33. E. M. Egorova and A. A. Revina, Kolloidn. Zh. **64**, 334 (2002) [Colloid. J. **64**, 301 (2002)].

34. E. M. Egorova, Zh. Fiz. Khim. **84**, 713 (2010) [Russ. J. Phys. Chem. A **84**, 629 (2010)].
35. E. M. Egorova, A. A. Revina, B. V. Rumyantsev, et al., Zh. Prikl. Khim. **75**, 1620 (2003) [Russ. J. Appl. Chem. **75**, 1585 (2002)].
36. G. B. Sergeev, *Nanochemistry* (Mosk. Gos. Univ., Moscow, 2003) [in Russian].
37. A. Maitra, J. Phys. Chem. **88**, 5122 (1984).
38. B. H. Robinson, A. N. Khan-Lodhi, and T. Towey, in *Structure and Reactivity in Reverse Micelles*, Ed. by M.-P. Pileni (Elsevier, New York, 1989), p. 199.
39. Yu. L. Khmelnitsky, A. V. Kabanov, N. L. Klyachko, et al., in *Structure and Reactivity in Reverse Micelles*, Ed. by M.-P. Pileni (Elsevier, New York, 1989), p. 230.
40. M. Hirai, R. Kawai-Hirai, S. Yabuki, et al., J. Phys. Chem. **99**, 6652 (1995).
41. W. Zhang, X. Qiao, J. Chen, and H. Wang, J. Colloid Interface Sci. **302**, 370 (2006).
42. W. Zhang, X. Quaio, and J. Chen, Mater. Sci. Eng. B **142**, 1 (2007).
43. E. M. Egorova and A. A. Revina, Zh. Fiz. Khim. **77**, 1683 (2003) [Russ. J. Phys. Chem. A **77**, 1513 (2003)].
44. H. El Hajji, E. Nkhili, V. Tomao, and O. Dangles, Free Rad. Res. **49**, 303 (2006).
45. L. Mira, M. T. Fernandez, M. Santos, et al., Free Rad. Res. **36**, 1199 (2002).
46. O. M. Andersen, *Flavonoids: Chemistry, Biochemistry, and Applications* (C.H.I.P, 2005).
47. C. Petit, P. Lixon, and M.-P. Pileni, J. Phys. Chem. **97**, 12974 (1993).
48. M. Treuger, C. de Cointer, H. Remita, et al., J. Phys. Chem. **102**, 4310 (1998).
49. M.-P. Pileni, Langmuir **13**, 3266 (1997).
50. Z.-Y. Huang, G. Mills, and B. Hajek, J. Phys. Chem. **97**, 11542 (1993).
51. A. Henglein and D. Meisel, J. Phys. Chem. **102**, 8364 (1998).
52. X. Shen, Q. Yuan, H. Liang, et al., Science China B **46**, 387 (2003).